Journal of Medicinal Chemistry

Brief Article

Discovery of (*R*)-(2-fluoro-4-((-4-methoxyphenyl)ethynyl)phenyl) (3-hydroxypiperidin-1-yl)methanone (ML337), an mGlu3 Selective and CNS Penetrant Negative Allosteric Modulator (NAM)

Cody J. Wenthur, Ryan Morrsion, Andrew S Felts, Katrina A. Smith, Julie L. Engers, Frank W. Byers, J. Scott Daniels, Kyle A Emmitte, P. Jeffrey Conn, and Craig W Lindsley

J. Med. Chem., **Just Accepted Manuscript** • DOI: 10.1021/jm400439t • Publication Date (Web): 29 May 2013

Journal of Medicinal Chemistry is published by the American Chemical Society. 1155 Sixteenth Street N.W., Washington, DC 20036

Discovery of (*R*)-(2-fluoro-4-((-4-methoxyphenyl)ethynyl)phenyl) (3-hydroxypiperidin-1-yl)methanone (ML337), an $mGlu_3$ Selective and CNS Penetrant Negative Allosteric Modulator (NAM)

Cody J. Wenthur [‡,§,#], Ryan Morrison [‡,§,#], Andrew S. Felts[‡,§,#], Katrina A. Smith[‡,§,#], Julie L. Engers[‡,§,#], Frank W. Byers[‡,§,#], J. Scott Daniels [‡,§,#], Kyle A. Emmitte[‡,§,∥,#], P. Jeffrey Conn[‡,§,#], Craig W. Lindsley*[,‡,§,∥,#]

[‡]Department of Pharmacology, [§]Vanderbilt Center for Neuroscience Drug Discovery, [#]Vanderbilt Specialized Chemistry for Accelerated Probe Development (MLPCN), Vanderbilt University Medical Center, Nashville, Tennessee 37232, [∥]Department of Chemistry, Vanderbilt University, Nashville, Tennessee 37232.

KEYWORDS. Metabotropic glutamate receptor, $mGlu_3$, negative allosteric modulator (NAM), ML337, MLPCN probe

Supporting Information Placeholder

ABSTRACT: A multi-dimensional, iterative parallel synthesis effort identified a series of highly selective mGlu3 NAMs with sub-micromolar potency and good CNS penetration. Of these, ML337 resulted ($mGlu_3$ IC_{50} = 593 nM, $mGlu_2$ IC_{50} >30 μM) with B:P ratios of 0.92 (mouse) to 0.3 (rat). DMPK profiling and shallow SAR led to the incorporation of deuterium atoms to address a metabolic soft spot, which subsequently lowered both in vitro and in vivo clearance by >50%.

INTRODUCTION

G-protein-coupled metabotropic glutamate receptors (mGluRs) have emerged as new drug targets with potential for treatment of a range of CNS disorders.[1-4] Highly subtype-selective allosteric ligands have previously been developed for $mGlu_1$, $mGlu_4$, $mGlu_5$ and $mGlu_7$.[1-9] While the group II mGluRs ($mGlu_2$ and $mGlu_3$) are among the most highly studied of the mGluR subgroups, previous efforts were limited to group II mGluR ligands that act at both $mGlu_2$ and $mGlu_3$.[1-4,6] Recently, selective positive allosteric modulators for $mGlu_2$ have emerged, and demonstrated that $mGlu_2$ activation is responsible for the antipsychotic efficacy of $mGlu_{2/3}$ agonists.[6] However, despite major advances in understanding the functions of $mGlu_2$, $mGlu_3$ remains one of the least understood mGluR subtypes, due in large part to the lack of selective ligands.[1-9] Despite this, numerous studies indicate that $mGlu_3$ is the key mGluR subtype involved in glial-neuronal communication, and inhibition of $mGlu_3$ is hypothesized to have therapeutic utility in the treatment of cognitive disorders, schizophrenia, depression and Alzheimer's disease.[1-12] Therefore, our laboratory focused attention on the development of selective $mGlu_3$ negative allosteric modulators (NAMs) as probes to elucidate the role of $mGlu_3$ in vivo.

To date, only three $mGlu_3$ NAMs have been reported (Figure 1).[11-13] The first, RO4491533 (**1**), a dual $mGlu_2$/$mGlu_3$ NAM ($mGlu_2$ IC_{50} = 296 nM, $mGlu_3$ IC_{50} = 270 nM)

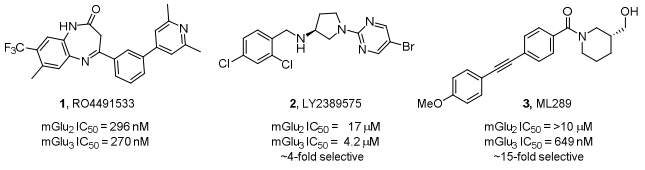

Figure 1. Structures and activities of reported mGlu3 NAMs 1-3.

was efficacious in cognition and depression models.[11] About the same time, Lilly disclosed LY2389575 (**2**), displaying ~4-fold selectivity for $mGlu_3$ over $mGlu_2$ ($mGlu_2$ IC_{50} = 17 μM, $mGlu_3$ IC_{50} = 4.2 μM).[12] In 2012, we disclosed a potent (IC_{50} = 649 nM), selective (>15-fold vs. $mGlu_2$) and CNS-penetrant $mGlu_3$ NAM (**3,** ML289), derived from a 0.37 μM $mGlu_5$ positive allosteric modulator (PAM).[13] Once again, a subtle 'molecular switch',[15] in the form of a *p*-methoxy moiety, conferred selective $mGlu_3$ inhibition over $mGlu_5$ potentiation. While this was a notable advance, we continued to seek an $mGlu_3$ NAM probe that was devoid of $mGlu_2$ activity (IC_{50} >30 μM) in order to enable proof of concept studies.

RESULTS AND DISCUSSION

Chemistry. **3** became our lead compound from which to develop a more potent and selective $mGlu_3$ NAM.[13] As we have previously reported, due to the steep nature of allosteric modulator SAR (especially in series prone to 'molecular switches'), we pursued an iterative parallel synthesis approach for the chemical optimization of **3**, [2,12,13] which was divided into five quadrants for SAR exploration

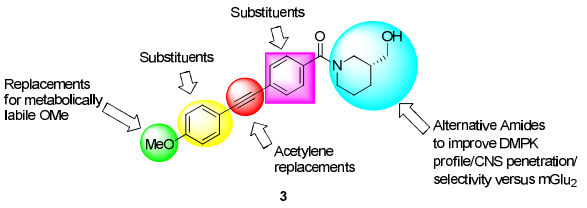

Figure 2. Library optimization strategy for **3** to improve $mGlu_3$ NAM activity, eliminate $mGlu_2$ activity and improve the DMPK profile.

(Figure 2). First, we wanted to identify replacements for the metabolically labile *p*-OMe moiety to improve improve disposition.[13] Second, we hoped to employ the wealth of acetylene replacements from previous $mGlu_5$ NAM discovery efforts to replace this less than optimal moiety.[8] Third, we desired to perform a broader amide scan to identify novel amide congeners that eliminate $mGlu_2$ activity. Finally, we wanted to see if the 'fluorine walk' approach[2] would offer advantages in terms of potency, selectivity or DMPK profiles.

Scheme 1. Synthesis of Aryl Analogues 6[a]

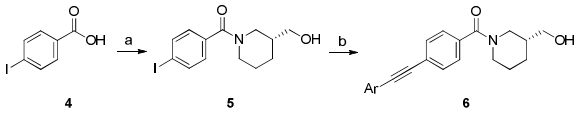

[a]Reagents and conditions: (a) (*R*)-3-hydroxymethyl piperidine, EDC, DMAP, DCM, DIPEA, 95%; (b) 20 mol% CuI, 5 mol% $Pd(PPh_3)_4$, arylacetylene (1.1 equiv.), DMF, DIEA, 60 °C, 1 h, 15-90%.

The first libraries were aimed at identifying a replacement for the *p*-methoxy moiety or electronically perturbing the aryl ring, rendering P450-mediated *O*-dealkylation less facile.[13] Following the synthetic route depicted in Scheme 1, a library of 24 analogs was readily prepared via standard amide and Sonogashira couplings, and screened against both $mGlu_3$ and $mGlu_2$ in kinetic assays (See supplemental information). All compounds possessed purity exceeding 95% as judged by ^1H NMR and analytical LCMS (214 nM, 254 nM and ELSD). SAR in this region was found to be shallow, as all attempts to increase steric bulk on the ether or electronically deactivate the aromatic ring (Figure 3) led to a significant loss of $mGlu_3$ activity (IC_{50}s >10 μM); thus the *p*-methoxy moiety was discovered to be an essential component of the biarylacetylene pharmacophore.

From the literature regarding acetylene replacements in related $mGlu_5$ NAM biaryl acetylene ligands, we synthesized and screened a diverse array of reported bioisosteres (Figure 4);[8] unfortunately, only a few weak NAMs were identified, with most inactive ($mGlu_3$ IC_{50}s >10 μM). Therefore, the *p*-methoxy phenyl acetylene component was crucial for $mGlu_3$ activity.

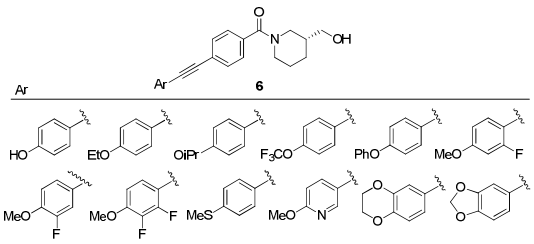

Figure 3. Representative Ar moieties surveyed to replace the *p*-OMe phenyl group. All lost significant activity against $mGlu_3$ (IC_{50}s >10 μM).

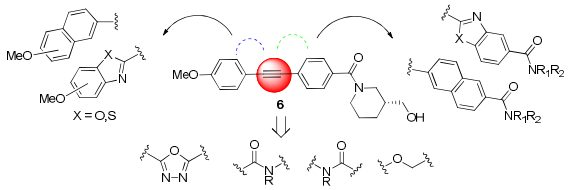

Figure 4. Representative acetylene biosiosteres surveyed to replace the *p*-OMe phenyl acetylene group.[8] All were weak to inactive on $mGlu_3$ (IC_{50}s >10 μM).

Based on these data, we elected to survey alternative amide moieties in an effort to improve $mGlu_3$ NAM activity and selectivity while holding the *p*-OMe phenyl acetylene pharmacophore constant. Key acid **7** was readily prepared by Sonogashira coupling as shown in Scheme 1, and amide analogues were prepared in high yield under standard conditions (Scheme 2).[13,15] This library proved far more productive, yielding a number of active analogues, and for the first time, robust SAR and a general lack of activity at $mGlu_2$ (Table 1).

Scheme 2. Synthesis of Amide Analogues 8[a]

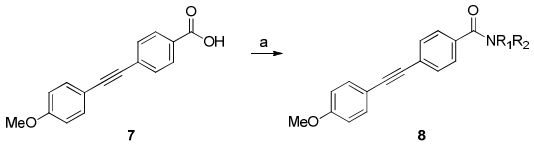

[a]Reagents and conditions: (a) HNR_1R_2, EDC, DMAP, DIPEA, CH_2Cl_2, rt, 16 h, 70-95%.

A racemic 3-hydroxy piperidine congener (**8a**) showed significant activity ($mGlu_3$ IC_{50} = 760 nM), and upon synthesis of the pure enantiomers, enantioselective inhibi-

tion was noted. Here, the (*R*)-enantiomer (**8d**) was more potent ($mGlu_3$ IC_{50} = 650 nM) than the (*S*)-enantiomer (**8c**, $mGlu_3$ IC_{50} = 1.1 μM). When the hydroxy group was capped as a methyl ether in **8**b, $mGlu_3$ NAM activity was lost. Interestingly, the [3.3.0] piperidine mimetic was active (**8k** and **8l**), and was a reasonably effective surrogate for the piperidine ring. Contraction to a pyrrolidine ring, as in **8g-i**, led to a significant diminution in potency, as did an acyclic congener **8f**. Based on the potency of the tertiary hydroxyl analogue **8j** (IC_{50} = 711 nM), we prepared the ethyl and allyl congeners as well, and resolved the enantiomers via chiral SFC.[15] Only modest ~2-fold increases in $mGlu_3$ NAM potency were noted for the (+)-enantiomers (Supplemental Figure 1). Finally, following the synthetic routes depicted in scheme 1 and 2, we incorporated fluorine atoms into the benzoic acid moiety of **8d**, and discovered two additional sub-micromolar $mGlu_3$ NAMs **9** and **10** worthy of further profiling (Figure 5).[15]

Table 1. Structures and Activities of Analogues 8.

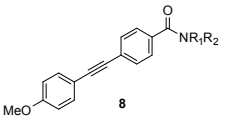

Entry	NR_1R_2	$mGlu_3$ pIC_{50}*	Glu Min* (%)	$mGlu_2$ IC_{50} (μM)
8a		5.87±0.04	0.4±3.0	>30
8b		5.26±0.05	0.0±3.2	>30
8c		5.77±0.04	1.7±3.2	>30
8d		6.18±0.02	2.0±1.5	>30
8f		5.12±0.11	1.6±39.8	>30
8g		4.56±1.61	---	>30
8h		4.99±0.09	0.0±16.1	>30
8i		5.12±0.11	0.0±10.3	>30
8j		5.96±0.06	-0.1±4.4	>30
8k		5.56±0.07	1.6±5.9	>30
8l		5.26±0.11	1.7±11.2	>30

*$mGlu_3$ pIC_{50} and Glu Min data reported as averages ±SEM from our calcium mobilization assay; n = 3

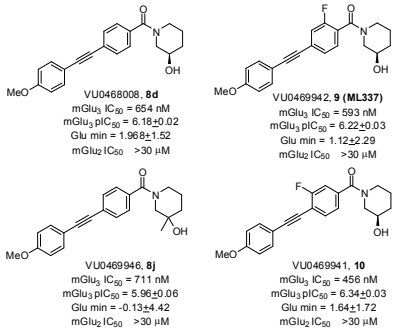

Figure 5. Potent and selective $mGlu_3$ NAMs for further profiling.

Molecular Pharmacology. The four leading $mGlu_3$ NAMs **8d**, **8j**, **9** and **10** proved to be potent and highly selective versus $mGlu_2$ (Figure 6). Based on DMPK and ancillary pharmacology profiles (*vide infra*), **9** was favored for further characterization. As shown in Figure 6C, **9**

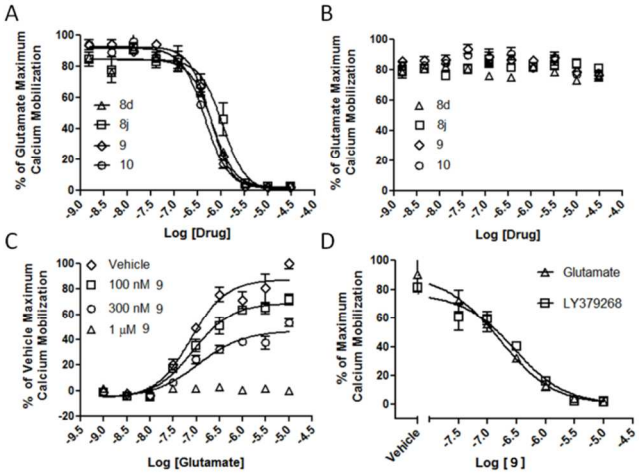

Figure 6. Molecular pharmacology profile of **9** and related $mGlu_3$ NAMs. A) $mGlu_3$ EC_{80} antagonist CRC. All four compounds are potent and fully efficacious $mGlu_3$ NAMs (n = 3). B) $mGlu_2$ EC_{80} CRC. All four compounds are inactive up to 30 μM. C) Progressive fold shift analysis with **9** and glutamate displayed a non-competitive decrease in the EC_{80}, indicating **9** is acting allosterically. D) Evaluating probe dependence. **9** is equipotent and efficacious in inhibiting $mGlu_3$ activation by both glutamate and LY379268 (Supplemental Figure 2).

displayed classical non-competitive antagonism with respect to the orthosteric agonist glutamate in a progressive fold shift assay.[2,3,13,15] For certain electrophysiology studies, an exogenous agonist may be required in order to engender selective group II mGluR activation; we therefore examined the probe dependence of **9**, and noted no differences between glutamate and LY379268[16] (Figure 6D). Considering **9** was inactive against the remaining mGluRs (no activity at $mGlu_{1,2,4,5,6,7,8}$ up to 30 μM) we declared ML337 an MLPCN probe.[17]

DMPK Disposition Attributes. **9** was subsequntly profiled in a battery of *in vitro* and *in vivo* DMPK assays to assess its utility as *in vivo* probe (Table 2). Although **9** was found to be unstable in rat and human microsomes,

it possessed free fractions in both mouse and human plasma approaching 0.03 (97% PPB), as well as a favorable P_{450} inhibition profile and solubility (7.8 μM in PBS). In a Ricerca radioligand binding panel of 68 GPCRs, ion channels and transporter,[18] displayed significant activity (>50% inhibition @10 μM) at only 2 targets (DAT, 71% and 5-HT_{2B}, 74%), but no functional activity at these targets. To rapidly assess the extent of CNS penetration, we performed a mouse tissue distribution study in which **8b**, **8j**, **9**, and **10** were administered as a cassette via an IP route, followed by LC/MS/MS analysis of plasma and brain tissue. All four compounds afforded acceptable CNS exposure, producing brain-to-plasma ratios (B:P) ranging from 0.59 to 0.92 in mice (Supplemental Table 1). **9** demonstrated a B:P ratio approaching unity (B:P, 0.92), with a $Brain_{AUC}$ of 3.37 μM and a corresponding $plasma_{AUC}$ of 3.71 μM. A subsequent rat study demonstrated a good overall CNS exposure for **9**, producing a B:P ratio of 0.3 with high plasma exposures (Supplemental Table 2).

Table 2. DMPK Characterization of ***9***

Parameter	*9*
MW	353.38
TPSA	59.7
cLogP	3.51
In Vitro Pharmacology	***IC_{50} (μM)***
CYP (1A2, 2C9, 3A4, 2D6)	>30, >30, >30, >30
In Vitro PK	
Rat CL_{HEP} (mL/min/kg)	54.1
Human CL_{HEP} (mL/min/kg)	18.9
Rat PPB (f_u)	0.005
mPPB (f_u)	0.027
In Vivo Rat PK (IP, 10 mg/kg, 0-6 h)	
Plasma AUC_{0-6} (μM*h)	33.1
Brain AUC_{0-6} (μM*h)	9.6
Brain:Plasma	0.3

The major metabolite of **9**, as with **3**, was P450-mediated *O*-demethylation.[14] As mentioned above, all efforts to replace this group synthetically proved futile, resulting in inactive compounds. In an attempt to improve the PK in rodents, we elected to introduce deuterium atoms into the methoxy substituent (D_3) of both **8d** and **9** in order to increase the metabolic stability of these mGlu3 NAMs (providing **11** and **12**, respectively).[19] As shown in Table 3, introduction of the D_3CO moitety led to an analog with a substantially lower intrinsic clearance (CL_{int}) and predicted hepatic clearance value (CL_{hep}) in vitro. Indeed, the deuteration strategy resulted in an approximate 50% lowering of the plasma clearance (CL_p) in rats while providing $mGlu_3$ NAMs of comparable potency and selectivity (Supplemental Figure 3). Importantly, identification of the principal metabolites of the deuterated analogs revealed there to be no metabolic shunt from P_{450}-mediated *O*-demethylation (data not shown). Thus, employing the apparent kinetic isotope effect as a means to combat the shallow SAR of these allosteric modulators led to improved disposition in vivo.[19]

Conclusion. In summary, we have developed the most potent ($mGlu_3$ IC_{50} = 593 nM, 1.9% Glu min) and selective (>30 μM versus $mGlu_{1,2,4,5,6,7,8}$) $mGlu_3$ NAM, **9**, described to date. ML337 possesses a favorable DMPK and ancillary pharmacology profile, and is centrally penetrant. The major metabolic soft spot was identified to be P450-mediated *O*-demethylation, a fate that could not be overcome through standard steric or electronic perturbations, due to extremely shallow allosteric ligand SAR. However,

Table 3. Effect of deuterium incorporation on in vitro and in vivo rat PK with **8d** and **9**.

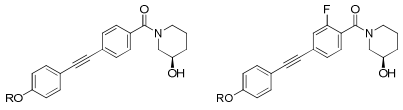

	R = CH_3 **8d**	R = CD_3 **11**	R = CH_3 **9**	R = CD_3 **12**
Rat CL_{INT} (mL/min/kg)	214	97.3	239	73.7
Rat CL_{HEP} (mL/min/kg)	52.7	40.7	54.1	35.9
Rat IV PK CL_p (mL/min/kg)	6.2	3.3	5.2	2.9
Rat IV PK V_{ss} (L/kg)	0.22	0.21	0.21	0.18
$mGlu_3$ IC_{50} (μM)	0.65	0.31	0.59	0.45

by exploiting apparent kinetic isotope effects, we were able to combat the shallow SAR within this allosteric modulator series and discover an mGlu3 NAM with improved disposition. Electrophysiology and in vivo studies with **9**, and its deuterated analogue **12**, are in progress and will be reported in due course.

EXPERIMENTAL SECTION

Chemistry. The general chemistry, experimental information, and syntheses of all other compounds are supplied in the Supporting Information. **(*R*)-(2-Fluoro-4-((4-methoxyphenyl)ethynyl)(3-hydroxypiperdin-1-yl)methanone, 9:** To a solution of 2-fluoro-4-((4-methoxyphenyl) ethynyl) benzoic acid (675 mg, 2.5 mmol) in 20 mL DMF, was added DIPEA (1.07 g, 8.25 mmol) while stirring. EDC (560 mg, 3 mmol), HOBt (337 mg, 2.5 mmol), and (*R*)-3-hydroxypiperidine hydrochloride (342 mg, 2.5 mmol) were then added. The reaction was allowed to stir for 4 hours at room temperature, then quenched with a solution of saturated $NaHCO_3$ (20 mL), washed with 5% LiCl (aqueous, 2 x 20 mL), and brine (20 mL). The reaction was extracted into dichloromethane (50 mL), and solvent was removed under vacuum. HPLC purification afforded **9** as an ivory solid (420 mg, 47%). ^1H

NMR (500 MHz, *d*6-DMSO, 75^0 C) δ (ppm): 7.50 (m, 2H); 7.39 (m, 3H); 6.99 (m, 2H); 4.06 (s, 1H); 3.82 (s, 3H); 3.53 (s, 1H); 3.29 (m, 2H); 2.93 (m, 1H); 1.87 (m, 1H); 1.74 (s, 1H); 1.44 (m, 2H). ^{13}C NMR (125 MHz, *d*6-DMSO, 75^0 C) δ (ppm): 163.3, 159.7, 158.0, 156.0, 132.7, 127.2, 125.2 (d, *J* = 9.3 Hz), 124.3 (d, *J* = 16.7 Hz), 117.7 (d, *J* = 22.7 Hz), 114.2, 113.4, 91.1, 85.9, 64.7, 55.0, 53.2, 48.2, 32.2, 28.9. $[\alpha]_D^{23}$ = -27.6^o (*c* = 1, MeOH). LC (254 nm) 0.704 min (>99%); MS (ESI) *m*/*z* = 354.1. HRMS (TOF, ES+) $C_{21}H_{20}FNO_3[M+H]^+$ calc. mass 354.1505, found 354.1507.

ASSOCIATED CONTENT

Supporting Information. Experimental procedures and spectroscopic data for selected compounds, detailed pharmacology and DMPK methods. This material is available free of charge via the Internet at http://pubs.acs.org.

Corresponding Author

*Phone: 615-322-8700. Fax: 615-343-3088. E-mail: craig.lindsley@vanderbilt.edu.

Funding Sources

This work was generously supported by the NIH/MLPCN U54 MH084659 (C.W.L.) and NIMH R01MH099269 (K.A.E).

ABBREVIATIONS USED

$mGlu_3$, metabotropic glutamate receptor subtype 3; CRC, concentration-response-curve; IP, intra-peritoneal; MLPCN, Molecular Libraries Probe Production Centers Network; RCF, relative centrifugal force

REFERENCES

(1) Conn, P.J.; Pin, J-P. Pharmacology and functions of metabotropic glutamate receptors. *Annu. Rev. Pharmacol. Toxicol.* **1997**, *37*, 205-237.

(2) Melancon, B.J.; Hopkins, C.R.; Wood, M.R.; Emmitte, K.A.; Niswender, C.M.; Christopoulos, A.; Conn, P.J.; Lindsley, C.W. Allosteric modulation of seven transmembrane spanning receptors: theory, practice, and opportunities for central nervous system drug discovery. *J. Med. Chem*. **2012**, 55, 1445-1464.

(3) Conn, P.J.; Christopolous, A.; Lindsley, C.W. Allosteric modulators of GPCRs: a novel approach for the treatment of CNS disorders. *Nat. Rev. Drug Discov*. **2009**, *8*, 41-54.

(4) Conn, P.J.; Lindsley, C.W.; Jones, C. Activation of metabotropic glutamate receptors as a novel approach for the treatment of schizophrenia. *Trends in Pharm. Sci.* **2009**, 30, 25-31.

(5) Robichaud, A.J.; Engers, D.W.; Lindsley, C.W.; Hopkins, C.R. Recent progress on the identification of metabotropic glutamate 4 receptor ligands and their potential utility as CNS therapeutics. *ACS Chem. Neurosci*. **2011**, *2*, 433-449.

(6) Sheffler, D.J.; Pinkerton, A.B.; Dahl, R.; Markou, A.; Cosford, N.D.P. Recent Progress in the Synthesis and Characterization of Group II Metabotropic Glutamate Receptor Allosteric Modulators. *ACS Chem. Neurosci*. **2011**, *2*, 382-393.

(7) Emmitte, K.A. Recent advances in the design and development of novel negative allosteric modulators of mGlu5. *ACS Chem. Neurosci*. **2011**, *2*, 411-432.

(8) Stauffer, S.R. Progress toward Positive Allosteric Modulators of the Metabotropic Glutamate Receptor Subtype 5 ($mGlu_5$). *ACS Chem. Neurosci.* **2011**, *2*, 450-470.

(9) Suzuki, G.; Tsukamoto, N.; Fushiki, H.; Kawagishi, A.; Nakamura, M.; Kurihara, H.; Mitsuya, M.; Ohkubo, M.; Ohta, H In vitro pharmacological characterization of novel isoxazolopyridone derivatives as allosteric metabotropic glutamate receptor 7 antagonists.. *J. Pharmacol. Exp. Ther.* **2007**, *323*, 147-156.

(10) Harrision, P.J.; Lyon, L.; Sartorius, L.J.; Burnet, P.W.J.; Lane, T.A The group II metabotropic glutamate receptor 3 (mGlu3, GRM3): expression, function and involvement in schizophrenia. *J. Psychopharm*. **2008**, *22*, 308-322.

(11) Campo, B.; Kalinichev, M.; Lambeng, N.; El Yacoubi, M.; Royer-Urios, I.; Schneider, M.; Legarnd, C.; Parron, D.; Girard, F.; Bessif, A.; Poli, S.; Vaugeois, J-M.; Le Poul, E.; Celanire, S. Characterization of an mGluR2/3 negative allosteric modulator in rodent models of depression. J. *Neurogenetics* **2011**, *24*, 152-166.

(12) Caraci, F.; Molinaro, G.; Battaglia, G.; Giuffrida, M.L.; Riozzi, B.; Traficante, A.; Bruno, V.; Cannella, M,.; Mero, S.; Wang, X.; Heinz, B.A.; Nisenbaum, E.S.; Britton, T.C.; Drago, F.; Sortino, M.A.; Copani, A.; Nicoletti, F. Targeting group II metabotropic glutamate (mGlu) receptors for the treatment of psychosis associated with Alzheimer's disease: selective activation of mGlu2 receptors amplifies beta-amyloid toxicity in cultured neurons, whereas dual activation of mGlu2 and mGlu3 receptors is neuroprotective. *Mol. Pharm.* **2011**, *79*, 618-626.

(13) Sheffler, D.J.; Wenthur, C.J.; Bruner, J.A.; Carrington, S.J.S.; Blobaum, A.L.; Morrison, R.D.; Daniels, J.S.; Niswender, C.M.; Conn, P.J.; Lindsley, C.W. Development of a novel, CNS penetrant metabotropic glutamate receptor 3 (mGlu3) NAM probe (ML289) derived from a closely related mGlu5 PAM. *Bioorg. Med. Chem. Lett*. **2012**, *22*, 3921-3925.

(14) Wood, M.R.; Hopkins, C.R.; Brogan, J.T.; Conn, P.J.; Lindsley, C.W. Molecular switches' on allosteric ligands that modulate modes of pharmacology. *Biochemistr*y **2011**, 50, 2403-2410.

(15) See Supporting Information for full details.

(16) Monn, J.A.; Valli, M.J.; Massey, S.M.; Hansen, M.M.; Kress T.J.; Wepsiec, J.P.; Harkness, A.R.; Grutsch, J.L.; Wright, R.A.; Johnson, B.G.; Andis, S.L.; Kingston, A.; Tomlinson, R.; Lewis, R.; Griffey, K.R.; Tizzano, J.P.; Schoepp, D.D. Synthesis, pharmacological characterization, and molecular modeling of heterobicyclic amino acids related to (+)-2-aminobicyclo[3.1.0]hexane-2,6-dicarboxylic acid (LY354740): identification of two new potent, selective, and systemically active agonists for group II metabotropic glutamate receptors. *J. Med. Chem*. **1999**, *42*, 1027–1040.

(17) For MLPCN, please see: http://mli.nih.gov/mli

(18) For information on Ricerca, see: www.ricerca.com

(19) Nelson, S.D.; Trager, W.F. The use of deuterium isotope effects to probe the active site properties, mechanism of cytochrome P450-catalyzed reactions, and mechanisms of meta-

bolically dependent toxicity. *Drug Metab. Dispos.* **2003**, *31*, 1481–1498.

TABLE OF CONTENTS GRAPHIC

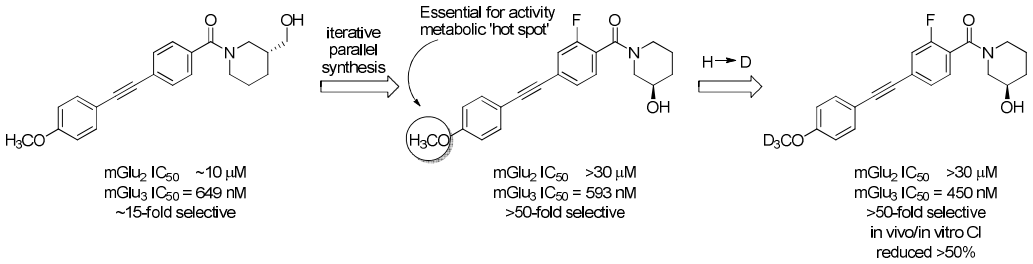

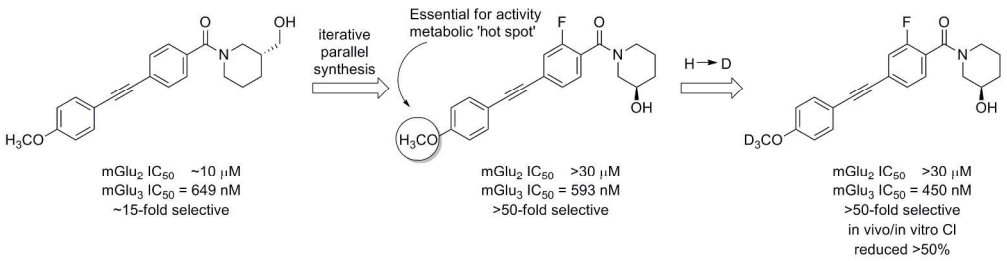

237x61mm (300 x 300 DPI)

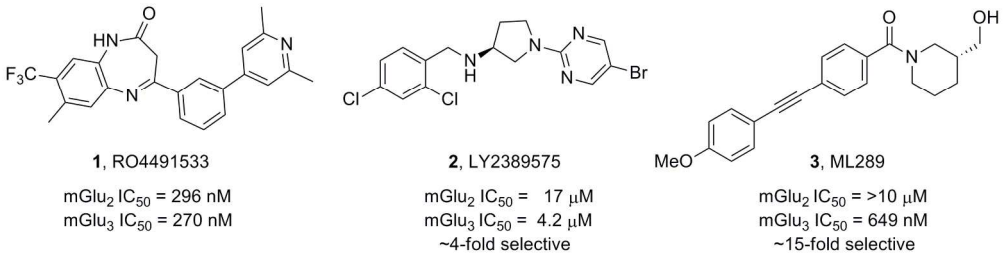

195x50mm (300 x 300 DPI)

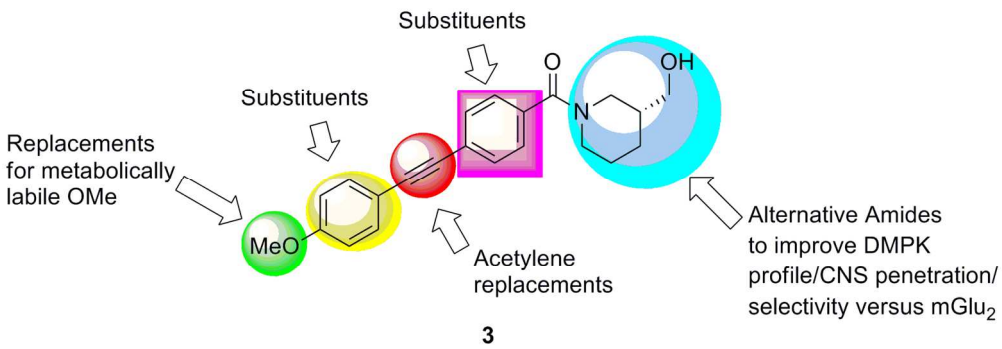

3

151x53mm (300 x 300 DPI)

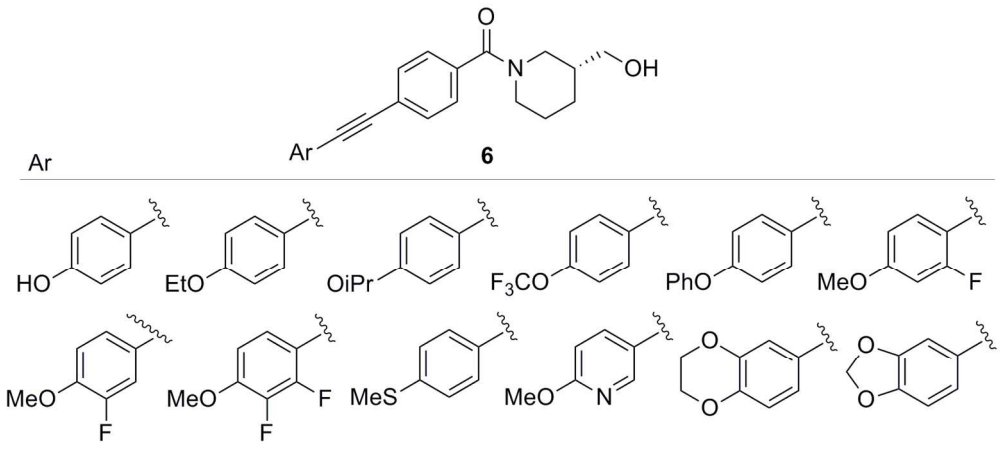

149x66mm (300 x 300 DPI)

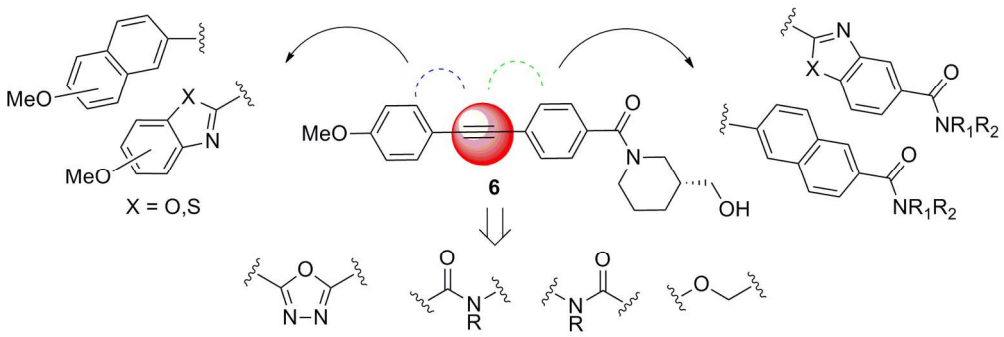

164x54mm (300 x 300 DPI)

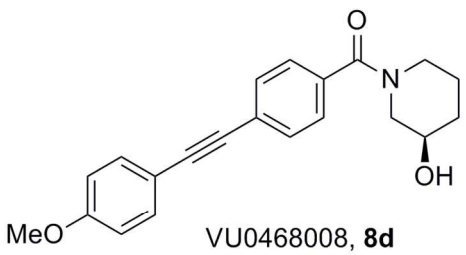

VU0468008, **8d**
$mGlu_3$ IC_{50} = 654 nM
$mGlu_3$ pIC_{50} = 6.18±0.02
Glu min = 1.968±1.52
$mGlu_2$ IC_{50} >30 μM

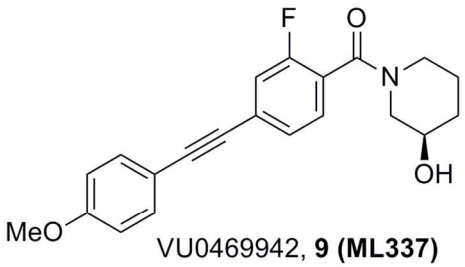

VU0469942, **9 (ML337)**
$mGlu_3$ IC_{50} = 593 nM
$mGlu_3$ pIC_{50} = 6.22±0.03
Glu min = 1.12±2.29
$mGlu_2$ IC_{50} >30 μM

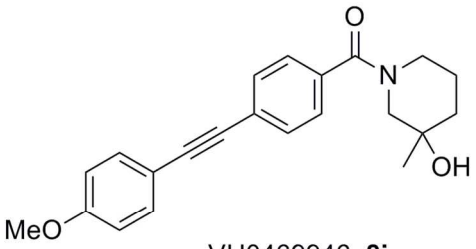

VU0469946, **8j**
$mGlu_3$ IC_{50} = 711 nM
$mGlu_3$ pIC_{50} = 5.96±0.06
Glu min = -0.13±4.42
$mGlu_2$ IC_{50} >30 μM

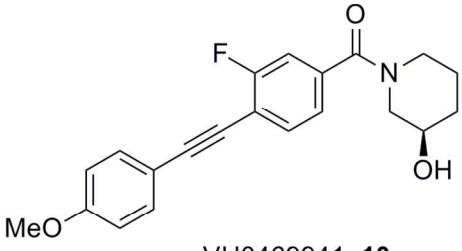

VU0469941, **10**
$mGlu_3$ IC_{50} = 456 nM
$mGlu_3$ pIC_{50} = 6.34±0.03
Glu min = 1.64±1.72
$mGlu_2$ IC_{50} >30 μM

130x109mm (300 x 300 DPI)

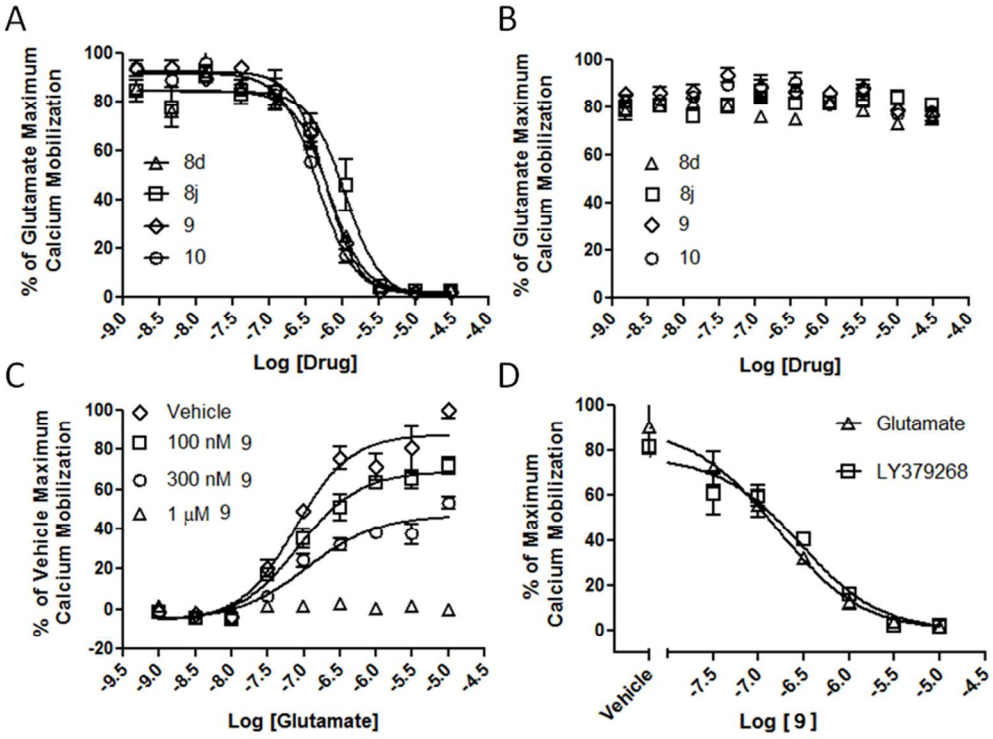

249x185mm (96 x 96 DPI)

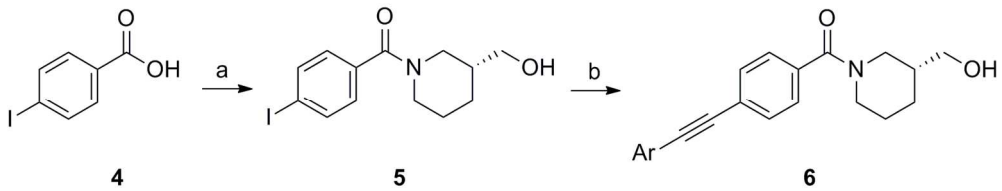

4 **5** **6**

151x29mm (300 x 300 DPI)

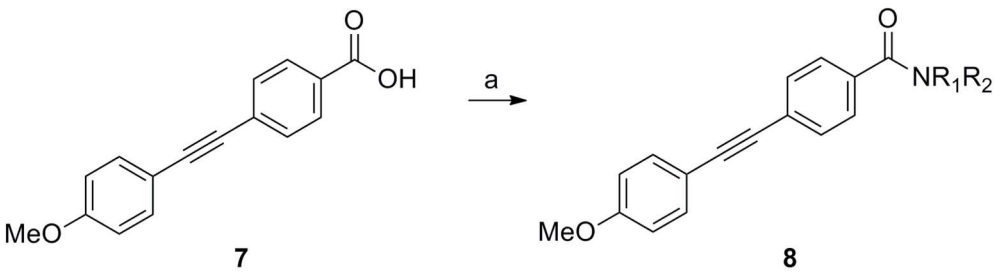

130x36mm (300 x 300 DPI)

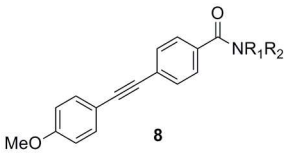

8

Entry	NR_1R_2	$mGlu_3$ pIC_{50}*	Glu Min* (%)	$mGlu_2$ IC_{50} (μM)
8a		5.87±0.04	0.4±3.0	>30
8b		5.26±0.05	0.0±3.2	>30
8c		5.77±0.04	1.7±3.2	>30
8d		6.18±0.02	2.0±1.5	>30
8f	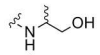	5.12±0.11	1.6±39.8	>30
8g		4.56±1.61	---	>30
8h		4.99±0.09	0.0±16.1	>30
8i	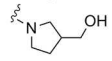	5.12±0.11	0.0±10.3	>30
8j		5.96±0.06	-0.1±4.4	>30
8k		5.56±0.07	1.6±5.9	>30
8l	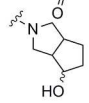	5.26±0.11	1.7±11.2	>30

*$mGlu_3$ pIC_{50} and Glu Min data reported as averages±SEM from our calcium mobilization assay; n = 3

119x243mm (300 x 300 DPI)

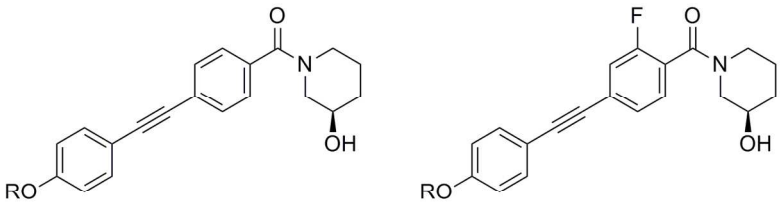

	R = CH_3,**8d**	R = CD_3, **11**	R = CH_3, **9**	R = CD_3, **12**
Rat CL_{INT} (mL/min/kg)	214	97.3	239	73.7
Rat CL_{HEP} (mL/min/kg)	52.7	40.7	54.1	35.9
Rat IV PK CL_p (mL/min/kg)	6.2	3.3	5.2	2.9
Rat IV PK V_{ss} (L/kg)	0.22	0.21	0.21	0.18
$mGlu_3$ IC_{50} (μM)	0.65	0.31	0.59	0.45

159x104mm (300 x 300 DPI)